Hsp90 inhibitor 17-AAG reduces ErbB2 levels and inhibits proliferation of the trastuzumab resistant breast tumor cell line JIMT-1

Barbara Zsebik [a], Ami Citri [b], Jorma Isola [c], Yosef Yarden [b], János Szöllősi [a,d], György Vereb [a,*]

[a] *Department of Biophysics and Cell Biology, Faculty of Medicine, Medical and Health Science Centre,*
University of Debrecen, Debrecen, Hungary
[b] *Department of Biological Regulation, The Weizmann Institute of Science, Rehovot, Israel*
[c] *Institute of Medical Technology, University of Tampere, Tampere, Finland*
[d] *Cell Biophysics Research Group of the Hungarian Academy of Sciences, Research Centre for Molecular Medicine, Faculty of Medicine,*
Medical and Health Science Centre, University of Debrecen, Debrecen, Hungary

Abstract

ErbB2, a member of the EGF receptor family of tyrosine kinases is overexpressed on many tumor cells of epithelial origin and is the molecular target of trastuzumab (Herceptin), the first humanized antibody used in the therapy of solid tumors. Trastuzumab, which is thought to act, at least in part, by downregulating ErbB2 expression is only effective in ~30–40% of ErbB2 positive breast tumors. Geldanamycin and its derivative 17-AAG are potential antitumor agents capable of downregulating client proteins of Hsp90, including ErbB2. To investigate the ability of 17-AAG to downregulate ErbB2 in trastuzumab resistant breast cancer cells and the possibility of 17-AAG and trastuzumab potentiating each other's effect, the recently established trastuzumab resistant breast cancer cell line, JIMT-1 was compared to the known trastuzumab sensitive SKBR-3 line. Baseline and stimulus-evoked dimerization and activation levels of ErbB2, and the effects of trastuzumab and 17-AAG alone and in combination on cell proliferation and apoptosis, as well as on ErbB2 expression and phosphorylation have been measured. Baseline activation and amenability to activation and downregulation by trastuzumab was much lower in the resistant line. However, 17-AAG enhanced ErbB2 homodimerization after 5–10 min of treatment in both cell lines, and decreased proliferation with an IC_{50} of 70 nM for SKBR-3 and 10 nM for JIMT-1. Thus, 17-AAG may be a useful drug in trastuzumab resistant ErbB2 overexpressing tumors. The antiproliferative effect of 17-AAG was positively correlated with phosphorylation and downregulation of ErbB2 and was dominated by apoptosis, although, especially at higher doses, necrosis was also present. Interestingly, IC_{50} values for ErbB2 downregulation and phosphorylation, in the 30–40 nM range, were not significantly different for the two cell lines. This observation and the negative correlation between resting ErbB2 levels and the antiproliferative effect of 17-AAG may indicate that activation of ErbB2 to some extent could counteract the overall cytostatic effect, especially at higher levels of ErbB2 expression. The usual therapeutic dose of trastuzumab did not change the IC_{50} of 17-AAG on the proliferation of either cell line, but nevertheless decreased overall ErbB2 phosphorylation and at low doses of 17-AAG further decreased cell growth in the sensitive SKBR-3, thus trastuzumab may be a good combination partner to counteract undesired activating effects of 17-AAG.
© 2005 Elsevier B.V. All rights reserved.

Keywords: Breast tumor immunotherapy; Trastuzumab; 17-AAG; ErbB2

1. Introduction

ErbB2 is a member of the ErbB receptor tyrosine kinase family. Although it has no soluble high-affinity ligand [1], it fulfills a central role in the ErbB signal transducing network by increasing the ligand binding spectrum and affinity of ErbB1, 3 and 4, the other members of the family [2,3]. Activation of the ErbB family members requires their homo- or heterodimerization which is followed by transphosphorylation and downstream signaling cascades leading to cell proliferation and survival [4,5]. A most mitogenic heterodimer is formed of ErbB2 and ErbB3, the latter, though kinase deficient, serving as a receptor for neuregulins [6,7]. ErbB2-containing heterodimers are internalized less efficiently [8,9] and evade lysosomal degradation [10], an effect

* Corresponding author at: Department of Biophysics and Cell Biology, Faculty of Medicine, Medical and Health Science Centre, University of Debrecen, H-4012 Debrecen, Nagyerdei Krt. 98, P.O. Box 39, Hungary.
Tel.: +36 52 412623; fax: +36 52 412623.
E-mail address: vereb@dote.hu (G. Vereb).

which is even more pronounced upon ErbB2 overexpression [11], also leading to ligand-independent constitutive activation of ErbB2 homodimers [12,13].

ErbB2 is overexpressed in 25–30% of human breast cancers, and is associated with very poor prognosis [14]. Overexpressed membrane proteins, especially those – like ErbB2 – that are scarce in differentiated cells are ideal targets of molecular therapy. ErbB2 was the first antigen on a solid tumor to be targeted with a humanized monoclonal antibody, trastuzumab (Herceptin) [15,16]. Other molecular therapies targeting ErbB2 include the humanized 2C4 antibody (omnitarg) that inhibits ErbB2 dimerization [17,18] and the pan-ErbB kinase inhibitor CI-1033 [19], that are now investigated in several clinical trials.

While the use of trastuzumab in antibody-based cancer therapy has dynamically expanded over the past years, it also had to be realized that as single agent, it is ineffective in 60–70% of ErbB2 overexpressing breast tumors [20]. Even though trastuzumab, when combined with chemotherapy gives better initial results [21], continued administration of the antibody usually leads to secondary resistance. The molecular mechanisms of resistance to trastuzumab, similarly to its mode of action, are largely unknown and possibly include various factors. Autocrine production of EGF-like ligands [22] or overexpression of insulin-like growth factor 1 receptor (IGF1R) [23], leading to an ErbB2-independent means for the constitutive activation of the PI3K pathway, as well as blocking of trastuzumab binding by MUC4, a cell surface mucin [24,25], have been implicated in trastuzumab resistance.

Trastuzumab binds to a membrane-proximal domain of ErbB2 [26,27] and causes partial activation and internalization of the receptor [28]. Although the internalization itself may not be a definitive requirement for the antiproliferative effect of trastuzumab [29,30], decreased cell surface ErbB2 levels could well be one distinct cause of decreased cell proliferation [31]. Thus, in the clinical setting, it could be a reasonable approach to use alternative methods to decrease ErB2 levels of overexpressing, but trastuzumab resistant tumor cells.

The chaperon Hsp90, besides catalyzing the proper folding of newly synthesized client proteins into a stable tertiary conformation, has been implicated in the stabilization of a number of cellular proteins that play central roles in signal transduction processes [32]. ErbB2, alone in the ErbB family, possesses a sequence in its kinase domain that is responsible for Hsp90 binding [33,34]. Interestingly, binding of Hsp90 to ErbB2 not only serves to maintain its physiological conformation, but also to restrain ErbB2 from forming active signaling dimers [35].

Ansamycin antibiotics isolated from *Streptomyces hygroscopicus* [36], such as geldanamycin, were found to inhibit the growth of many cancer cell lines at nanomolar concentrations [37]. Geldanamycin having a very narrow therapeutic window [38], more promising analogs such as 17-(allylamino)-17-demethoxygeldanamycin (17-AAG) were synthesized. 17-AAG exhibited decreased toxicity and enhanced stability, and even though its binding to Hsp90 was weaker than that of geldanamycin, 17-AAG displayed an antitumor effect similar to geldanamycin [39,40]. It also proved to be reasonably success-

ful in phase I clinical trials in spite of formulation problems and side effects [41], especially in two cases of melanoma [42].

Among several signaling molecules (such as Raf-1, CDK4, Lck), 17-AAG was found to decrease ErbB2 levels in breast [39,43], prostate [44] and ovarian [45] cancer cells. However, it remains unclear to what extent downregulation of ErbB2 levels is correlated with the antiproliferative effect of 17-AAG, and whether it would also be effective in the cases where trastuzumab does not effectively decrease cell surface ErbB2 levels and proliferation. Furthermore, it is of importance to learn whether in trastuzumab sensitive tumors 17-AAG and trastuzumab could be used together to potentiate each others effect.

In this study we have exploited the recently established first trastuzumab resistant breast cancer cell line, JIMT-1, that can be passaged in vitro [46] and compared these cells to the known trastuzumab sensitive SKBR-3 line. We investigated baseline and stimulated dimerization and activation levels of ErbB2, and the effects of trastuzumab and 17-AAG alone and in combination on cell proliferation and apoptosis, as well as on ErbB2 expression and phosphorylation. Our results indicate that while baseline activation and amenability to activation and downregulation by trastuzumab is much lower in the resistant line, its proliferation is more prone to inhibition by 17-AAG. In both cell lines, the antiproliferative effect of 17-AAG was correlated with the downregulation of ErbB2. The usual therapeutic dose of trastuzumab did not change the IC_{50} of 17-AAG on the proliferation of either cell line, but nevertheless decreased overall ErbB2 phosphorylation and at low doses of 17-AAG further decreased cell growth in the sensitive SKBR-3.

2. Materials and methods

2.1. Cell cultures and reagents

SKBR-3 was obtained from the American Type Culture Collection (ATCC, Manassas, VA), whereas the JIMT-1 breast tumor cell line [46] was isolated at the University of Tampere. SKBR-3 cells were cultured in a humidified atmosphere with 5% CO_2 at 37 °C in Dulbecco's minimal essential medium (DMEM) supplemented with 10% fetal calf serum and antibiotics. JIMT-1 cells were grown in a 1:1 mixture of DMEM and Ham's F-12 similarly to SKBR-3. Cells were propagated every 3–4 days using 0.05% trypsin and 0.02% EDTA. For microscopy experiments, cells were seeded onto 12 mm diameter glass coverslips or on Lab-Tek[TM] II chambered coverglass (Nalge Nunc International, Rochester, NY) 2 days in advance and used at a confluence of 30–50%. For flow cytometric measurements cells were harvested with trypsinization. Before stimulation experiments, the cultures were starved in serum-free DMEM for 24 h.

Natural murine EGF was obtained from IC Chemikalien (Ismaning, Germany). 17-(allylamino)-17-demethoxygeldanamycin (17-AAG) was a kind gift of Kosan Biosciences Inc. (Hayward, CA), and stored as a 10 mM stock solution in DMSO at −20 °C. All other chemicals, unless indicated otherwise, were from Sigma (Schnelldorf, Germany).

2.2. Antibodies

The mouse monoclonal antibody 2C4 against ErbB2 was a kind gift from Genentech Inc. (South San Francisco, CA). Trastuzumab was from Hoffman-La Roche AG (Germany). The mouse monoclonal antibody AB18 (clone PN2A) against the activated phospho-form of ErbB2 was from Lab Vision, Fremont, CA. The antibody 528 against ErbB1 was isolated from the supernatant of the corresponding hybridoma line (American Type Culture Collection, Rockville, MD, Cat # HB-8509) using protein-C beads (Sigma). These antibodies were conjugated with sulfoindocyanine dyes Cy3 and Cy5 (monofunctional succinimidyl ester, Amersham, Piscataway, NJ) or Alexa-488 (Invitrogen, Carlsbad, CA) according to the manufacturers' instructions.

2.3. Flow cytometric determination of ErbB2 expression and phosphorylation

To determine the expression level and phosphorylation state of ErbB2, 8×10^5 cells from each treatment group were trypsinized, blocked with medium containing 10% FCS, washed three times with Hepes buffered saline (HBS) (7 min, $600 \times g$) and divided into two aliquots, one for background control, the other for labeling. Extracellular ErbB2 was labeled in 100 μl volume of 20 μg/ml Cy5-2C4 for 10 min at 4 °C. After washing in HBS, samples were fixed in 300 μl of 1% formaldehyde for 20 min at 4 °C. Fixation was followed by incubation in HBS with 1% milk powder, 0.1% saponin and 1 mM sodium-*ortho*-vanadate for 20 min at room temperature. Samples were washed, and P-ErbB2 was labeled in 100 μl volume with 10 μg/ml Alexa-488 conjugated Ab-18 for 40 min at room temperature in HBS with 1% milk powder, 0.1% saponin and 1 mM sodium-*ortho*-vanadate. Samples were washed and fixed in 500 μl 1% formaldehyde. Fluorescence was measured in a FACSCalibur flow cytometer (Becton Dickinson, Franklin Lakes, NJ) using excitation wavelengths of 488 and 635 nm and detecting emissions through 520 and 661 nm bandpass (FL1, FL4). A total of 10,000 events were recorded in list mode after logarithmic amplification of the fluorescence signal. The mean of fluorescence histograms was corrected for the mean of the corresponding blank control. ErbB2 expression was calibrated using the known expression level of viable SKBR-3 cells, which was determined to be 800,000 using QIFIKIT (DakoCytomation, Glostrup, Denmark) according to the manufacturer's instructions.

2.4. Measuring ErbB2 homo- and heteroassociation

Cells grown to 80% confluence on coverslips were treated with 40 μg/ml trastuzumab or 50 nM EGF in 50 μl HBS in a wet chamber at 37 °C for 7 min, or with 0.5 μM 17-AAG in 50 μl HBS for 2, 5 or 10 min. Coverslips were washed in ice cold HBS, fixed for 5 min in 1% formaldehyde, washed three times, and cell were labeled for fluorescence resonance energy transfer measurements. For measuring ErbB2–ErbB2 homoassociation, ErbB2 was labeled with 20 μg/ml Cy3-2C4 as donor and 20 μg/ml Cy5-2C4 as acceptor (mixed in advance)

in 50 μl HBS with 1% BSA at 4 °C for 10 min. For determining ErbB1–ErbB2 heteroassociation, the same procedure was used, but as donor 20 μg/ml Cy3-528 was used against ErbB1. Finally the samples were washed again and mounted in 5 μl Mowiol (0.1 M Tris–HCl, pH 8.5, 25% (w/v) glycerol, and 10% Mowiol 4–88, Hoechst Pharmaceuticals, Frankfurt, Germany) on pre-cleaned microscopic slides.

Fluorescence resonance energy transfer (FRET) efficiency was measured using the acceptor photobleaching protocol (for details see [47]). Briefly, in the molecular proximity of an acceptor fluorophor emission from the donor is decreased. Photobleaching the acceptor releases the donor from this quenching which results in increased fluorescence intensity. The FRET efficiency E in each pixel of the microscopic image can be calculated as

$$E_{(i,j)} = 1 - \frac{F_{D(i,j)}^{\mathrm{I}}}{\gamma F_{D(i,j)}^{\mathrm{II}}} \tag{1}$$

where $F_{D(i,j)}^{\mathrm{I}}$ and $F_{D(i,j)}^{\mathrm{II}}$ are the background subtracted donor fluorescence values of the (i,j)th pixel in the entire image before (I) and after (II) photobleaching the acceptor. In the denominator, γ is a correction factor that takes into consideration the photobleaching of the donor during the whole protocol. It can be calculated as

$$\gamma = \frac{\left\langle F_{D(i,j)}^{\mathrm{ref,I}} \right\rangle}{\left\langle F_{D(i,j)}^{\mathrm{ref,II}} \right\rangle} \tag{2}$$

where $\left\langle F_{D(i,j)}^{\mathrm{ref,I}} \right\rangle$ and $\left\langle F_{D(i,j)}^{\mathrm{ref,II}} \right\rangle$ are the mean, background subtracted donor intensities in pixels above threshold of a reference sample labeled with donor only, before (I) and after (II) running an identical acceptor photobleaching protocol.

The measurement protocol was implemented in an LSM 510 confocal microscope (Carl Zeiss, Göttingen, Germany) using a Plan Apochromat 63×/1.4 NA objective. Cy3 was excited with a 543 nm HeNe laser and detected through a 560–605 nm bandpass filter. Cy5 was excited with a 633 nm HeNe laser and detected through a 650 longpass filter. 512×512 pixel images were acquired in multi-track mode to avoid crosstalk between channels using extended depth of focus (open pinhole). A custom C script was written and used with SCIL Image (TNO, Amsterdam, The Netherlands) to evaluate image sequences and calculate average FRET efficiency according to Eqs. (1) and (2) for pixels above threshold in each frame, usually containing 2–5 cells.

2.5. Assessing cell proliferation

The effect of 17-AAG, and trastuzumab alone and in combination on cell proliferation was tested in a protocol of daily treatment for 4 days, starting 24 h after seeding 4000 cells/well into 96-well plates. 17-AAG alone was used at concentrations of 0.0005; 0.005; 0.05; 0.5 and 1.7 μM, and trastuzumab alone at doses of 2; 10; 40; 100 and 200 μg/ml. The same doses of 17-AAG were also combined with 40 μg/ml trastuzumab. Sepa-

rate plates were prepared for measuring cell numbers after each day of treatment. A tetrazolium based assay (EZ4U, Biomedica Medizinprodukte GmbH and Co KG, Wien, Austria) was used according to the manufacturer's instructions. Cells were grown in 200 μl indicator-free medium, 20 μl of the dye solution was added to each well and incubated for 6 h (SKBR-3) or 4 h (JIMT-1) at 37 °C. Absorbance was measured at 450 and 620 nm with an ELISA reader and the OD^{corr} parameter characteristic of cell number was calculated as

$$OD^{corr} = OD_{450} - OD_{620} \frac{OD^{ref}_{450}}{OD^{ref}_{620}} \tag{3}$$

where OD_{450} and OD_{620} are the optical densities measured at 450 and 620 nm for the tetrazolium treated samples, and OD^{ref}_{450} and OD^{ref}_{620} are their equivalents for unstained controls.

Readings for each data point were taken in triplicate. A calibration curve OD^{corr} versus cell number was obtained by freshly seeding a dilution series of cells and allowing them to adhere for 4 h. The time of incubation for each cell type was optimized in a time series for various seeded cell numbers so that numbers observed during the proliferation assay were covered linearly by the parameter OD^{corr}.

For measuring ErbB2 expression levels and ErbB2 phosphorylation at the end of 4 days of treatment, cells were seeded at 10^4 cm^{-2} into 5 cm Petri dishes and subjected to the same treatment protocols.

2.6. Quantifying apoptosis

Annexin V-FITC Apoptosis Detection Kit (Sigma APO-AF) was applied to determine the extent of apoptosis in 17-AAG-treated SKBR-3 and JIMT-1 cells. 10^4 cells/well were cultured in 8-well Nunc chamber slides in 400 μl indicator-free medium. Cells were treated daily with 0; 0.005; 0.05 and 0.5 μM 17-AAG for four consecutive days. After the treatment, cells were incubated with 400 μl of a binding buffer (100 mM HEPES/NaOH, 1.4 M NaCl and 25 mM CaCl2, pH 7.5) containing 0.2 μM Annexin V-FITC and 0.8 μM propidium iodide for 10 min at room temperature. Images of each well were taken with a 40×/0.6 NA objective using an LSM 510 laser scanning microscope in tile mode. Excitation was at 488 and 543 nm, emission through 505–555 and 560–605 nm bandpass filters. The transmitted light image during 488 nm excitation was also recorded. Apoptotic (Anexin-V positive) and necrotic (only PI positive) cells were counted and normalized to total area.

3. Results

3.1. Dimerization and activation status of ErbB2 in SKBR-3 and JIMT-1

Since dimerization or higher order oligomerization is accepted as a key event in receptor tyrosine kinase activation, we have first examined the homo- and heterodimerization of ErbB2 on both SKBR-3 and JIMT-1 cells (Fig. 1A). The microscopic acceptor photobleaching approach allowed inves-
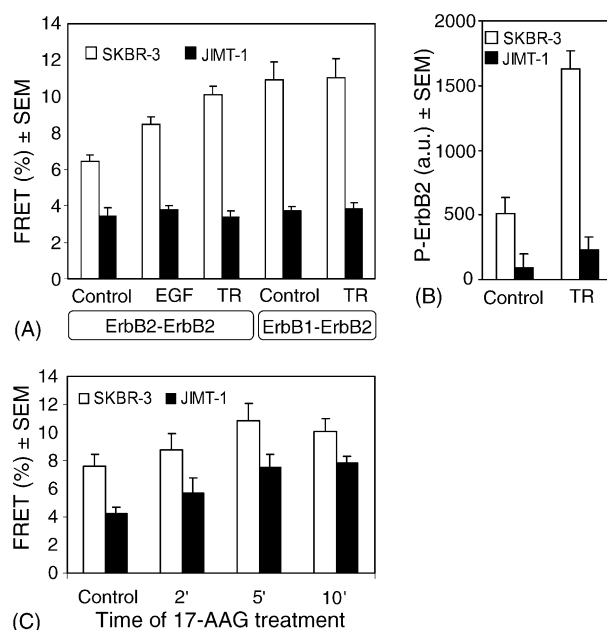

Fig. 1. Dimerization and phosphorylation of ErbB2 in trastuzumab sensitive and resistant cells. (A) FRET efficiency measured by microscopic acceptor photobleaching between ErbB1–ErbB2 or ErbB2–ErbB2 pairs on SKBR-3 and JIMT-1 cells in quiescence or after 50 nM EGF (+EGF) or 40 μg/ml trastuzumab (+TR) treatment for 7 min. Mean ± S.E.M. of >5 independent measurements. (B) Baseline and trastuzumab-induced (7 min, 40 μg/ml) ErbB2 phosphorylation measured by flow cytometry in JIMT-1 and SKBR-3. Mean ± S.E.M. of three independent histogram means. (C) ErbB2 homodimerization in SKBR-3 and JIMT-1 after 2, 5 and 10 min treatment with 0.5 μM 17-AAG measured by microscopic acceptor photobleaching. Mean ± S.E.M. of >5 independent measurements.

tigating the cells in their native, adherent state. In JIMT-1 cells, ErbB2–ErbB2 homoassociation was very low, and EGF (50 nM) or trastuzumab (40 μg/ml) did not have any effect on it. SKBR-3 cells exhibited a higher basal level of ErbB2 homoassociation, which was further increased by EGF and even more so by trastuzumab treatment. ErbB1–ErbB2 heteroassociation was high on SKBR-3, and as low on JIMT-1 as ErbB2 homoassociation. Trastuzumab had no effect on the ErbB1–ErbB2 heterodimers on either cell lines.

Flow cytometric measurements indicated that the low dimerization level of ErbB2 in JIMT-1 was paralleled by a low level of ErbB2 phosphorylation, which increased to a small extent upon treatment with 40 μg/ml trastuzumab as measured by flow cytometry (Fig. 1B). On the other hand, in SKBR-3, ErbB2 tyrosine phosphorylation was higher, and increased to over 300% upon trastuzumab treatment.

As a next step, 17-AAG was used to assess whether inhibiting Hsp90 can revert this low dimerization and activation state of ErbB2 in JIMT-1. As shown in Fig. 1C, 0.5 μM 17-AAG significantly increased ErbB2 homoassociation both in JIMT-1 and SKBR-3 cells; the effect peaked at 5 min after adding the drug and was maintained at least for another 5 min. These observations indicate that 17-AAG could be used to promote activation and internalization of ErbB2 not only in SKBR-3, but also in the trastuzumab resistant JIMT-1.

3.2. Cell proliferation in the presence of trastuzumab, 17-AAG, and their combination

Dose–response curves of trastuzumab and 17-AAG were determined for the proliferation of both SKBR-3 and JIMT-1 cells (Fig. 2). 2–200 μg/ml trastuzumab was added to the cells daily, while 17-AAG was given at concentrations of 0.0005–1.7 μM, also for four consecutive days. In the case of SKBR-3, concentrations as low as 40 μg/ml for trastuzumab (Fig. 2A) and 0.05 μM for 17-AAG (Fig. 2B) inhibited cell proliferation starting from the third day. According to expec-

tations, trastuzumab had negligible effect on the proliferation of JIMT-1 cells at the therapeutic 40 μg/ml concentration, and had only little effect compared to SKBR-3 even at 200 μg/ml (Fig. 2A). As opposed to this, 17-AAG at 0.05 μM concentration decreased proliferation of JIMT-1 even more than in SKBR-3 (Fig. 2B). In the case of SKBR-3, the effect of smaller doses (0.0005 and 0.005 μM) of 17-AAG were enhanced by 40 μg/ml trastuzumab, whereas higher doses were not significantly influenced by combining with them the antibody. In JIMT-1, the addition of trastuzumab to the 17-AAG regime appeared to cause no change in the proliferation rates (Fig. 2C).
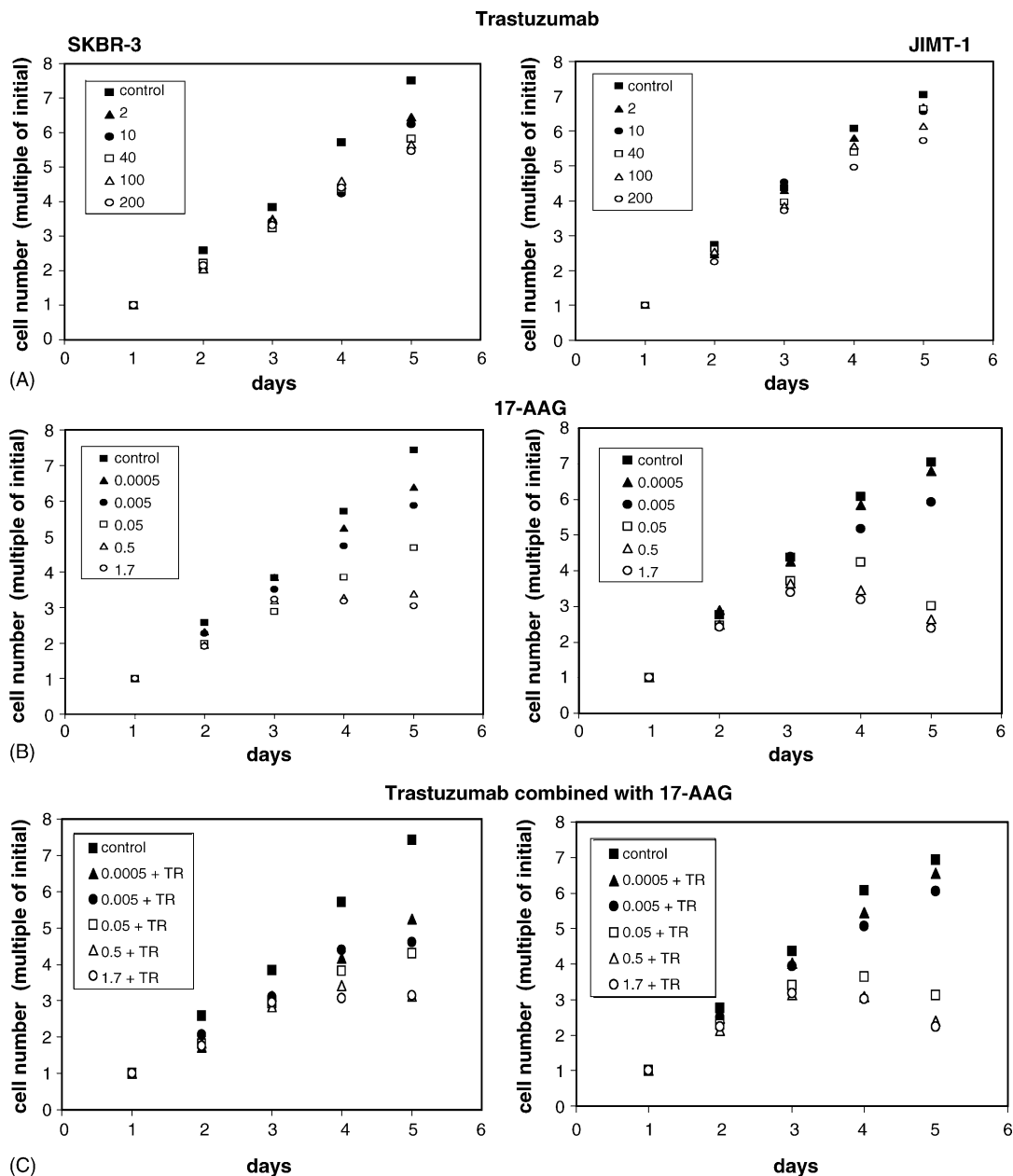

Fig. 2. Proliferation curves of SKBR-3 and JIMT-1 cells treated with trastuzumab, 17-AAG or their combination. Cell numbers determined from calibrated tetrazolium-based colorimetric assay are plotted as multiple of initially seeded cell counts. Means of three independent experiments. (A) Daily treatment with 0 μg/ml (■), 2 μg/ml (▲), 10 μg/ml (●), 40 μg/ml (□), 100 μg/ml (△) or 200 μg/ml (○) trastuzumab. (B) Daily treatment with 0 μM (■), 0.0005 μM (▲), 0.005 μM (●), 0.05 μM (□), 0.5 μM (△), or 1.7 μM (○) 17-AAG. (C) Combination of 0 μM (■), 0.0005 μM (▲), 0.005 μM (●), 0.05 μM (□), 0.5 μM (△), or 1.7 μM (○) 17-AAG and 40 μg/ml trastuzumab applied daily.

3.3. 17-AAG causes dose-dependent apoptosis and, to some extent, necrosis

To reveal the mechanisms behind the antiproliferative effect of 17-AAG, the amount of Anexin-V positive and propidium iodide (PI) positive cells was determined after 4 days of culture in the presence of 0.005, 0.05 and 0.5 μM 17-AAG and compared to the control (Fig. 3). Cells that displayed Anexin-V staining in the membrane were considered apoptotic regardless of PI positivity, whereas PI positive cells with no Anexin-V labeling were counted as necrotic. 17-AAG promoted both apoptosis and necrosis in a dose-dependent manner in both cell lines. Of the two processes, apoptosis was the dominant.

3.4. Dose-dependence of cell proliferation, ErbB2 membrane levels and ErbB2 phosphorylation upon 17-AAG treatment

To determine the half-effective concentration of 17-AAG, cells were treated for 4 days, administering 17-AAG daily in the dose range 0.0005–1.7 μM, either alone, or in combination with 40 μg/ml trastuzumab. At day 5, the number of cells per well was determined using a tetrazolium-based colorimetric assay, and the number of ErbB2 molecules in the membrane of cells, as well as the amount of phospho-ErbB2 in the cells was determined by flow cytometry. The dose-dependence of measured parameters showed typical sigmoid curves (Fig. 4A and B) that
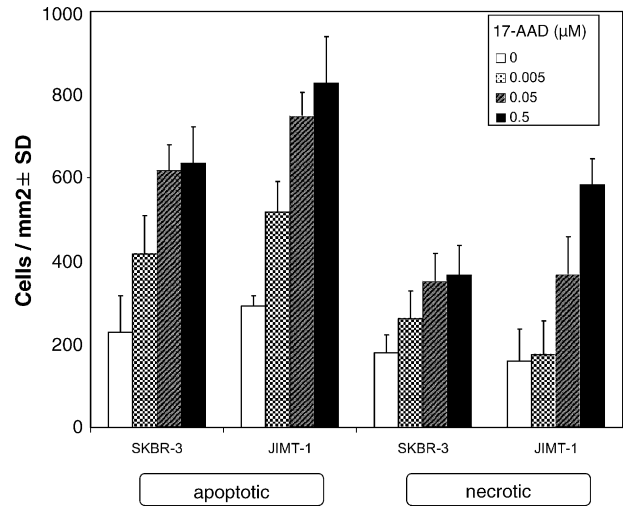

Fig. 3. Dose-dependence of apoptosis and necrosis in 17-AAG treated cells. The number of Anexin-V positive cells/mm^2 signifies apoptosis, whereas the number of PI positive cells/mm^2 signifies necrosis. JIMT-1 and SKBR-3 cells were treated with 0.005, 0.05, and 0.5 μM 17-AAG. Data are mean ± S.D. of three independent measurements.

were fitted to the Hill equation to obtain IC$_{50}$ values (Table 1). JIMT-1 cells were more sensitive to 17-AAG than SKBR-3 in terms of proliferation (Fig. 4A), with IC$_{50}$ values of 0.011 μM as opposed to 0.069 μM in the latter. Addition of therapeutic dose of trastuzumab appeared to cause a minor increase in the IC$_{50}$
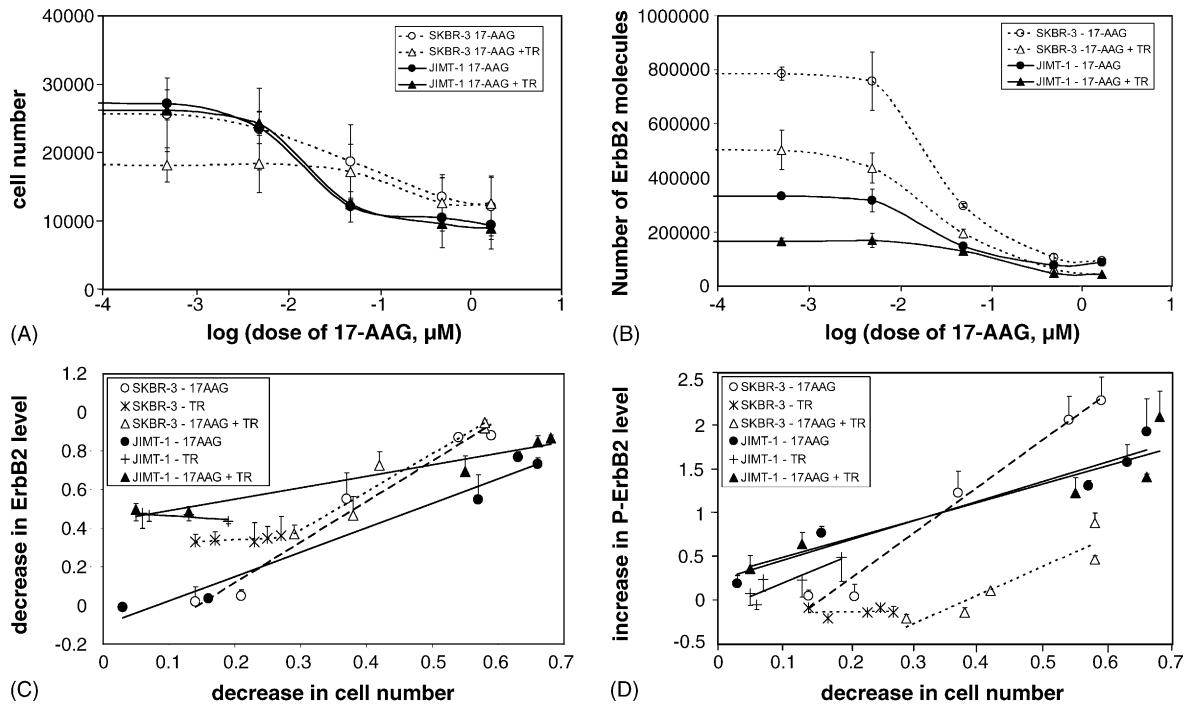

Fig. 4. Effect of 17-AAG and its combination with trastuzumab on ErbB2 expression, P-ErbB2 levels and cell proliferation. ErbB2 expression, P-ErbB2 levels and the number of cells was measured after 4 days of daily treatment with 2, 10, 40, 100 or 200 μg/ml trastuzumab, or 0.0005, 0.005, 0.05, 0.5, or 1.7 μM 17-AAG, or the combination of 0.0005, 0.005, 0.05, 0.5, or 1.7 μM 17-AAG and 40 μg/ml trastuzumab. Data are mean ± S.D. of three independent experiments. (A and B) Dose response curves of 17-AAG alone or in combination with 40 μg/ml trastuzumab. (A) Cell numbers on day 5 as a function of 17-AAG dose. (B) Number of ErbB2 molecules in the cell membrane as a function of 17-AAG dose. (C and D) Correlation plots of cytostatic effect and ErbB2 or P-ErbB2 levels. Cytostatic effect is expressed as decrease of cell number normalized to control. (C) Decrease of cell surface ErbB2 levels is expressed as 1-(ErbB2 count after treatment/ErbB2 count in control). (D) Increase of ErbB2 phosphorylation is expressed as (P-ErbB2 immunofluorescence normalized to that in the control)-1. Negative values mean decreased phosphorylation relative to control.

Table 1
Half-effective concentrations (IC_{50}) of 17-AAG alone and in combination with trastuzumab

IC_{50} (μM)	Proliferation		ErbB2 level		P-ErbB2 level	
	SKBR-3	JIMT-1	SKBR-3	JIMT-1	SKBR-3	JIMT-1
17-AAG	0.069 ± 0.011	0.011 ± 0.003	0.029 ± 0.001	0.028 ± 0.002	0.044 ± 0.007	0.036 ± 0.009
17-AAG (+TR)	0.086 ± 0.063	0.018 ± 0.004	0.022 ± 0.002	0.08 ± 0.013	0.331 ± 0.090	0.031 ± 0.008

IC_{50} values were determined from fitting dose–response curves to the Hill equation. Data $\pm$ S.D. are derived from three independent experiments. R^2 values were ≥ 0.995. +TR indicates the presence of 40 μg/ml trastuzumab in addition to increasing doses of 17-AAG.

of 17-AAG (Table 1). In the case of SKBR-3, IC_{50} of 17-AAG was not changed by adding trastuzumab to the cells, but at low 17-AAG doses, where the effect of the chaperon inhibitor was not very pronounced, 40 μg/ml trastuzumab caused a significant decrease of proliferation as compared to treatment with 17-AAG alone.

As shown in Fig. 4B, cell surface levels of ErbB2 were equally well decreased by 17-AAG in SKBR-3 and JIMT-1, yielding IC_{50} values of ∼0.03 μM in both. ErbB2 numbers in JIMT-1 at 0 μM 17-AAG concentration were somewhat below 50% of those in SKBR-3, in coherence with previous data [24,25] and with Western blotting experiments (data not shown). Addition of 40 μg/ml trastuzumab to the cells had negligible effect on IC_{50} of 17-AAG in SKBR-3, but doubled it in JIMT-1 (Table 1). Also, trastuzumab alone decreased cell surface ErbB2 levels in both cell lines, even though it had no effect on the proliferation of JIMT-1.

Somewhat surprisingly, 17-AAG caused an increase in total phospho-ErbB2 levels in a dose-dependent manner both in SKBR-3 and in JIMT-1, in spite of the overall downregulation of membrane ErbB2. The half-effective doses were similar in both cell lines, ∼0.04 μM. Upon addition of trastuzumab, phospho-ErbB2 levels did not change in JIMT-1 as compared to 17-AAG-only treated cells. However, ErbB2 phosphorylation decreased to a great extent in SKBR-3, and the efficiency of 17-AAG in promoting phosphorylation decreased by an order of magnitude (Fig. 4D and Table 1).

3.5. Correlation of the antiproliferative effect of trastuzumab, 17-AAG and their combination with ErbB2 numbers and ErbB2 phosphorylation

Using the antiproliferative effect (decrease of cell number normalized to control), the decrease of ErbB2 expression normalized to control levels, and the increase of phospho-ErbB2 level normalized to control as readout parameters at the end of the five-day treatment period, the correlation between these parameters after treatment with trastuzumab, 17-AAG, or their combination was investigated (Fig. 4C and D). In both SKBR-3 and JIMT-1, the decrease of membrane ErbB2 levels correlated positively ($R^2 > 0.8$, $p < 0.05$) with the antiproliferative effect of 17-AAG, regardless of the presence or absence of trastuzumab. Trastuzumab alone inhibited the proliferation of SKBR-3 and decreased ErbB2 levels to ∼40%. In coherence with this, addition of trastuzumab to 17-AAG treated SKBR-3 cells shifted the ErbB2 decrease versus antiproliferative effect plot to greater starting values, but did not change its slope. While

trastuzumab hardly inhibited the proliferation of JIMT-1 at therapeutic concentration, it did decrease ErbB2 levels on these cells similarly to SKBR-3. In accordance with this, when 40 μg/ml trastuzumab was added to 17-AAG treated JIMT-1 cells, the starting point of the ErbB2 decrease versus antiproliferative effect plot did not change in terms of relative decrease in cell number, but was shifted towards more downregulated ErbB2 values.

There was positive correlation ($R^2 > 0.85$, $p < 0.05$) between the increase of phospho-ErbB2 levels and the antiproliferative effect of 17-AAG both in SKBR-3 and JIMT-1, regardless of whether 40 μg/ml trastuzumab was present or not. Furthermore, decrease of ErbB2 levels and increase of ErbB2 phosphorylation were also positively correlated in both cells (not shown, $R^2 > 0.8$, $p < 0.05$). Trastuzumab alone slightly increased ErbB2 phosphorylation of JIMT-1 cells in a dose-dependent manner, but did not change the correlation plot of increase of phospho-ErbB2 versus decrease of cell number in JIMT-1. In the case of SKBR-3, trastuzumab alone exerted a slight decreasing effect on phospho-ErbB2 levels which was independent of trastuzumab dose. Adding 40 μg/ml trastuzumab to 17-AAG treated cells had a most striking effect of reducing ErbB2 phosphorylation to below control levels in the case of 0.0005 and 0.005 μM 17-AAG, but also significantly decreasing phospho-ErbB2 at higher doses of 17-AAG, as compared to the same doses of 17-AAG applied alone. At the same time, the antiproliferative effect of 17-AAG was enhanced for low doses, and maintained for high doses.

4. Discussion

As opposed to SKBR-3, a known trastuzumab sensitive breast tumor cell line, the newly established trastuzumab resistant line JIMT-1 exhibits low basal levels of ErbB2–ErbB2 homo- and ErbB1–ErbB2 heterodimerization and ErbB2 activation. While in SKBR-3 trastuzumab or EGF increased ErbB2 homoassociation and phosphorylation, in JIMT-1 no significant changes of ErbB2 dimerization could be measured by fluorescence resonance energy transfer, and phospho-ErbB2 levels increased only to a small extent. The data on phosphorylation obtained using in situ immunofluorescent labelling and flow cytometry correlate well with Western blot measurements [24]. Trastuzumab had no effect on ErbB1–ErbB2 heterodimerization in either cell lines, coherent with recent findings using trastuzumab beads and measuring ErbB1 phosphorylation as a readout for activation [25], which, taken together, hint that trastuzumab probably does not favor ErbB heterodimer formation.

0.5 µM 17-AAG caused a similar time-dependent increase of ErbB2 homoassociation in both cell lines. This is coherent with the present concept that in JIMT-1 the decreased effectiveness of trastuzumab is probably owed to masking of the trastuzumab-binding extracellular epitope on ErbB2 [24], but otherwise ErbB2 is fully functional and can be activated if this steric hindrance is overcome, for example by using high local concentrations of trastuzumab coupled to paramagnetic microspheres [25]. The data also substantiate previous findings [35] that show increased heterodimerization of ErbB2 upon inhibition of Hsp90 by geldanamycin or 17-AAG and support the notion that Hsp90 restrains ErbB2 from forming active dimers. Taken together, 17-AAG could be used to promote activation and internalization of ErbB2 not only in SKBR-3, but also in the trastuzumab resistant JIMT-1.

Consequently, we have tested the effect of 17-AAG, trastuzumab, and their combination on the proliferation time-curves of SKBR-3 and JIMT-1 cells, and found that 17-AAG decreased cell proliferation in both cell lines by promoting both apoptosis and necrosis in a dose-dependent manner. Of the two processes, apoptosis was the dominant. JIMT-1 cells were more sensitive to 17-AAG than SKBR-3, with IC_{50} values of 0.011 µM as opposed to 0.069 µM in the latter. 17-AAG also decreased the number of cell surface ErbB2 molecules in both cells with equal IC_{50}. In spite of the overall downregulation of membrane ErbB2, 17-AAG caused an increase in total phospho-ErbB2 levels in a dose-dependent manner, with similar half-effective doses in both SKBR-3 and JIMT-1. There was significant positive correlation between the increase of phospho-ErbB2 levels and the antiproliferative effect, as well as between the decrease of ErbB2 levels and the antiproliferative effect in both SKBR-3 and JIMT-1 treated with 17-AAG. In spite of these positive correlations, the fact that the half-effective concentrations of 17-AAG are the same for the two cell lines in terms of regulating ErbB2 levels and phosphorylation, but are quite different in terms of antiproliferative effect indicates that we are probably looking at a dual effect. On the one hand, ErbB2 is released from inhibition by Hsp90, gets activated and downregulated. On the other hand, activated ErbB2 may also initiate survival and proliferation signals via the PI3K/Akt and MAP kinase pathways. Experimental evidence supporting this notion includes mutating the Hsp90 binding site of ErbB2, which allows higher rates of spontaneous ErbB2 activation and causes enhanced cell proliferation as compared to the wild type ErbB2 when transfected into NIH-3T3 cells [35]. Thus, the antiproliferative effect of 17-AAG likely relies on the downregulation of many other signaling molecules in addition to ErbB2, and in the case of higher levels of ErbB2 expression, such as SKBR-3 cells versus JIMT-1 cells, the more abundant survival and proliferation signals originating form Hsp90-free ErbB2 could cause the increase of IC_{50} values. Consequently, increased ErbB2 phosphorylation and decreased membrane ErbB2 levels are a good readout of dose-dependent 17-AAG effect, but cannot be the single cause of decreased proliferation. The phenomenon also calls for a more detailed investigation of how the different time schedules of administration would change the balance between antiproliferative and activating effect of 17-AAG, as this clearly would have ample clinical significance.

Trastuzumab alone did not affect the proliferation of JIMT-1 cells as expected based on its initial characterization [46], but inhibited the growth of SKBR-3 in the 2–200 µg/ml range. While trastuzumab at therapeutic dose had negligible antiproliferative effect in JIMT-1, it nevertheless decreased the cell surface ErbB2 expression and slightly increased ErbB2 phosphorylation in a dose-dependent manner. This finding may be related to a subpopulation of JIMT-1 that has much higher trastuzumab-binding capacity than average [24], and ErbB2 is therefore more effectively eliminated from its surface during trastuzumab treatment.

Addition of therapeutic dose of trastuzumab did not decrease the IC_{50} of 17-AAG on the proliferation of JIMT-1, in consistence with the negligible antiproliferative effect of trastuzumab in this cell line. Rather, a small increase of IC_{50} was observed in combination treatment. Furthermore, trastuzumab appeared to decrease the effectiveness of 17-AAG in downregulating ErbB2 on these cells, perhaps because trastuzumab bound to ErbB2 can recycle to the cell membrane avoiding immediate degradation [48].

In the case of SKBR-3, trastuzumab alone exerted a slight decreasing effect on phospho-ErbB2 levels, which was independent of trastuzumab dose. Adding 40 µg/ml trastuzumab to 17-AAG treated cells had a most striking effect in reducing ErbB2 phosphorylation to below control levels in the case of 0.0005 and 0.005 µM 17-AAG, but also significantly decreasing phospho-ErbB2 at higher doses of 17-AAG as compared to the same doses of 17-AAG applied alone. In terms of half-efficient dose, the ability of 17-AAG to promote ErbB2 phosphorylation in the presence of trastuzumab has decreased by an order of magnitude, while IC_{50} of 17-AAG on proliferation has not been changed. In fact, the antiproliferative effect of 17-AAG was enhanced for low doses, and maintained for high doses.

Taken together the effects of 17-AAG, trastuzumab and their combination in the trastuzumab resistant JIMT-1 and sensitive SKBR-3 lines, 17-AAG could become a useful therapeutic approach in the treatment of trastuzumab resistant, ErbB2 overexpressing tumors, but in our model system, application of trastuzumab combined with 17-AAG appears to have adverse effects in terms of downregulating ErbB2 and perhaps even in decreasing the IC_{50} of 17-AAG on cell proliferation. On the other hand, in trastuzumab sensitive tumors, especially with high levels of ErbB2 expression, 17-AAG could have a dual effect, both promoting and inhibiting cell proliferation. In these cases, additional trastuzumab in the treatment regime can be beneficial in terms of inhibiting 17-AAG-evoked ErbB2 phosphorylation and also in enhancing the growth inhibitory effects of low doses of 17-AAG. This result appears to be especially important in the context of clinical applications since from the only clinical trial currently investigating the efficacy of 17-AAG in breast tumors (see NCI Clinical Trials, http://www.cancer.gov/search/ViewClinicalTrials.aspx?cdrid=391198&protocolsearchid=1879469) those on concurrent trastuzumab therapy are excluded. In addition, ErbB2 being a potential target of 17-AAG, efforts have been made to synthesize 17-AAG—trastuzumab conjugates for specific

delivery of the chaperone inhibitor to ErbB2 overexpressing tumors [49]. Application of such conjugates also necessitates the proper knowledge of how 17-AAG and trastuzumab interact in tumors with various expression levels and diverse degrees of trastuzumab resistance.

Acknowledgements

References

[1] Klapper LN, Glathe S, Vaisman N, Hynes NE, Andrews GC, Sela M, et al. The ErbB-2/HER2 oncoprotein of human carcinomas may function solely as a shared coreceptor for multiple stroma-derived growth factors. Proc Natl Acad Sci USA 1999;96:4995–5000.
[2] Yarden Y, Sliwkowski MX. Untangling the ErbB signalling network. Nat Rev Mol Cell Biol 2001;2:127–37.
[3] Karunagaran D, Tzahar E, Liu N, Wen D, Yarden Y. Neu differentiation factor inhibits EGF binding. A model for trans-regulation within the ErbB family of receptor tyrosine kinases. J Biol Chem 1995;270:9982–90.
[4] Nagy P, Jenei A, Damjanovich S, Jovin TM, Szöllősi J. Complexity of signal transduction mediated by ErbB2: clues to the potential of receptor-targeted cancer therapy. Pathol Oncol Res 1999;5:255–71.
[5] Vereb G, Nagy P, Park JW, Szöllősi J. Signaling revealed by mapping molecular interactions: implications for ErbB-targeted cancer immunotherapies. Clin Appl Immunol Rev 2002;2:169–86.
[6] Tzahar E, Waterman H, Chen X, Levkowitz G, Karunagaran D, Lavi S, et al. A hierarchical network of interreceptor interactions determines signal transduction by Neu differentiation factor/neuregulin and epidermal growth factor. Mol Cell Biol 1996;16:5276–87.
[7] Citri A, Skaria KB, Yarden Y. The deaf and the dumb: the biology of ErbB-2 and ErbB-3. Exp Cell Res 2003;284:54–65.
[8] Wang Z, Zhang L, Yeung TK, Chen X. Endocytosis deficiency of epidermal growth factor (EGF) receptor-ErbB2 heterodimers in response to EGF stimulation. Mol Biol Cell 1999;10:1621–36.
[9] Lidke DS, Nagy P, Heintzmann R, Arndt-Jovin DJ, Post JN, Grecco H, et al. Quantum dot ligands provide new insights into ErbB/HER receptor-mediated signal transduction. Nat Biotechnol 2004;22:198–203.
[10] Lenferink AE, Pinkas-Kramarski R, van de Poll ML, van Vugt MJ, Klapper LN, Tzahar E, et al. Differential endocytic routing of homo- and hetero-dimeric ErbB tyrosine kinases confers signaling superiority to receptor heterodimers. Embo J 1998;17:3385–97.
[11] Worthylake R, Opresko LK, Wiley HS. ErbB-2 amplification inhibits downregulation and induces constitutive activation of both ErbB-2 and epidermal growth factor receptors. J Biol Chem 1999;274:8865–74.
[12] Di Fiore PP, Pierce JH, Kraus MH, Segatto O, King CR, Aaronson SA. ErbB-2 is a potent oncogene when overexpressed in NIH/3T3 cells. Science 1987;237:178–82.
[13] Lonardo F, Di Marco E, King CR, Pierce JH, Segatto O, Aaronson SA, et al. The normal ErbB-2 product is an atypical receptor-like tyrosine kinase with constitutive activity in the absence of ligand. New Biol 1990;2:992–1003.
[14] Slamon DJ, Clark GM, Wong SG, Levin WJ, Ullrich A, McGuire WL. Human breast cancer: correlation of relapse and survival with amplification of the HER-2/neu oncogene. Science 1987;235:177–82.
[15] Baselga J, Tripathy D, Mendelsohn J, Baughman S, Benz CC, Dantis L, et al. Phase II study of weekly intravenous recombinant humanized anti-p185HER2 monoclonal antibody in patients with HER2/neu-overexpressing metastatic breast cancer. J Clin Oncol 1996;14:737–44.
[16] Slamon DJ, Leyland-Jones B, Shak S, Fuchs H, Paton V, Bajamonde A, et al. Use of chemotherapy plus a monoclonal antibody against HER2 for metastatic breast cancer that overexpresses HER2. N Engl J Med 2001;344:783–92.
[17] Agus DB, Akita RW, Fox WD, Lewis GD, Higgins B, Pisacane PI, et al. Targeting ligand-activated ErbB2 signaling inhibits breast and prostate tumor growth. Cancer Cell 2002;2:127–37.
[18] Jackson JG, St Clair P, Sliwkowski MX, Brattain MG. Blockade of epidermal growth factor- or heregulin-dependent ErbB2 activation with the anti-ErbB2 monoclonal antibody 2C4 has divergent downstream signaling and growth effects. Cancer Res 2004;64:2601–9.
[19] Slichenmyer WJ, Elliott WL, Fry DW. CI-1033, a pan-ErbB tyrosine kinase inhibitor. Semin Oncol 2001;28:80–5.
[20] Vogel CL, Cobleigh MA, Tripathy D, Gutheil JC, Harris LN, Fehrenbacher L, et al. Efficacy and safety of trastuzumab as a single agent in first-line treatment of HER2-overexpressing metastatic breast cancer. J Clin Oncol 2002;20:719–26.
[21] Burris III H, Yardley D, Jones S, Houston G, Broome C, Thompson D, et al. Phase II trial of trastuzumab followed by weekly paclitaxel/carboplatin as first-line treatment for patients with metastatic breast cancer. J Clin Oncol 2004;22:1621–9.
[22] Motoyama AB, Hynes NE, Lane HA. The efficacy of ErbB receptor-targeted anticancer therapeutics is influenced by the availability of epidermal growth factor-related peptides. Cancer Res 2002;62:3151–8.
[23] Lu Y, Zi X, Zhao Y, Mascarenhas D, Pollak M. Insulin-like growth factor-I receptor signaling and resistance to trastuzumab (Herceptin). J Natl Cancer Inst 2001;93:1852–7.
[24] Nagy P, Friedländer E, Tanner M, Kapanen AI, Carraway KL, Isola J, et al. Decreased accessibility and lack of activation of ErbB2 in JIMT-1, a herceptin-resistant, MUC4-expressing breast cancer cell line. Cancer Res 2005;65:473–82.
[25] Friedländer E, Arndt-Jovin DJ, Nagy P, Jovin TM, Szöllősi J, Vereb G. Signal transduction of ErbB receptors in trastuzumab (Herceptin) sensitive and resistant cell lines: local stimulation using magnetic microspheres as assessed by quantitative digital microscopy. Cytometry A 2005;67:161–71.
[26] Nagy P, Bene L, Balázs M, Hyun WC, Lockett SJ, Chiang NY, et al. EGF-induced redistribution of ErbB2 on breast tumor cells: flow and image cytometric energy transfer measurements. Cytometry 1998;32:120–31.
[27] Cho HS, Mason K, Ramyar KX, Stanley AM, Gabelli SB, Denney Jr DW, et al. Structure of the extracellular region of HER2 alone and in complex with the Herceptin Fab. Nature 2003;421:756–60.
[28] Sarup JC, Johnson RM, King KL, Fendly BM, Lipari MT, Napier MA, et al. Characterization of an anti-p185HER2 monoclonal antibody that stimulates receptor function and inhibits tumor cell growth. Growth Regul 1991;1:72–82.
[29] Neve RM, Nielsen UB, Kirpotin DB, Poul MA, Marks JD, Benz CC. Biological effects of anti-ErbB2 single chain antibodies selected for internalizing function. Biochem Biophys Res Commun 2001;280:274–9.
[30] Nagy P, Vereb G, Sebestyén Z, Horváth G, Lockett SJ, Damjanovich S, et al. Lipid rafts and the local density or ErbB proteins influence the biological role of homo- and heteroassociations of ErbB2. J Cell Sci 2002;115:4251–62.
[31] Sliwkowski MX, Lofgren JA, Lewis GD, Hotaling TE, Fendly BM, Fox JA. Nonclinical studies addressing the mechanism of action of trastuzumab (Herceptin). Semin Oncol 1999;26:60–70.
[32] Pratt WB, Toft DO. Regulation of signaling protein function and trafficking by the hsp90/hsp70-based chaperone machinery. Exp Biol Med (Maywood) 2003;228:111–33.
[33] Xu W, Mimnaugh E, Rosser MF, Nicchitta C, Marcu M, Yarden Y, et al. Sensitivity of mature Erbb2 to geldanamycin is conferred by its kinase domain and is mediated by the chaperone protein Hsp90. J Biol Chem 2001;276:3702–8.

[34] Xu W, Yuan X, Xiang Z, Mimnaugh E, Marcu M, Neckers L. Surface charge and hydrophobicity determine ErbB2 binding to the Hsp90 chaperone complex. Nat Struct Mol Biol 2005;12:120–6.

[35] Citri A, Gan J, Mosesson Y, Vereb G, Szöllősi J, Yarden Y. Hsp90 restrains ErbB-2/HER2 signalling by limiting heterodimer formation. EMBO Rep 2004;5:1165–70.

[36] Uehara Y, Hori M, Takeuchi T, Umezawa H. Screening of agents which convert 'transformed morphology' of Rous sarcoma virus-infected rat kidney cells to 'normal morphology': identification of an active agent as herbimycin and its inhibition of intracellular src kinase. Jpn J Cancer Res 1985;76:672–5.

[37] Neckers L, Schulte TW, Mimnaugh E. Geldanamycin as a potential anticancer agent: its molecular target and biochemical activity. Invest New Drug 1999;17:361–73.

[38] Supko JG, Hickman RL, Grever MR, Malspeis L. Preclinical pharmacologic evaluation of geldanamycin as an antitumor agent. Cancer Chemother Pharmacol 1995;36:305–15.

[39] Schulte TW, Neckers LM. The benzoquinone ansamycin 17-allylamino-17-demethoxygeldanamycin binds to HSP90 and shares important biologic activities with geldanamycin. Cancer Chemother Pharmacol 1998;42:273–9.

[40] Kelland LR, Sharp SY, Rogers PM, Myers TG, Workman P. DT-diaphorase expression and tumor cell sensitivity to 17-allylamino, 17-demethoxygeldanamycin, an inhibitor of heat shock protein 90. J Natl Cancer Inst 1999;91:1940–9.

[41] Workman P. Combinatorial attack on multistep oncogenesis by inhibiting the Hsp90 molecular chaperone. Cancer Lett 2004;206:149–57.

[42] Banerji U, O'Donnell A, Scurr M, Pacey S, Stapleton S, Asad Y, et al. Phase I pharmacokinetic and pharmacodynamic study of 17-allylamino, 17-demethoxygeldanamycin in patients with advanced malignancies. J Clin Oncol 2005;23:4152–61.

[43] Tikhomirov O, Carpenter G. Geldanamycin induces ErbB-2 degradation by proteolytic fragmentation. J Biol Chem 2000;275:26625–31.

[44] Solit DB, Zheng FF, Drobnjak M, Munster PN, Higgins B, Verbel D, et al. 17-Allylamino-17-demethoxygeldanamycin induces the degradation of androgen receptor and HER-2/neu and inhibits the growth of prostate cancer xenografts. Clin Cancer Res 2002;8:986–93.

[45] Smith V, Hobbs S, Court W, Eccles S, Workman P, Kelland LR. ErbB2 overexpression in an ovarian cancer cell line confers sensitivity to the HSP90 inhibitor geldanamycin. Anticancer Res 2002;22:1993–9.

[46] Tanner M, Kapanen AI, Junttila T, Raheem O, Grenman S, Elo J, et al. Characterization of a novel cell line established from a patient with Herceptin-resistant breast cancer. Mol Cancer Ther 2004;3:1585–92.

[47] Vereb G, Matkó J, Szöllősi J. Cytometry of fluorescence resonance energy transfer. Meth Cell Biol 2004;75:105–52.

[48] Austin CD, De Maziere AM, Pisacane PI, van Dijk SM, Eigenbrot C, Sliwkowski MX, et al. Endocytosis and sorting of ErbB2 and the site of action of cancer therapeutics trastuzumab and geldanamycin. Mol Biol Cell 2004;15:5268–82.

[49] Mandler R, Kobayashi H, Hinson ER, Brechbiel MW, Waldmann TA. Herceptin-geldanamycin immunoconjugates: pharmacokinetics, biodistribution, and enhanced antitumor activity. Cancer Res 2004;64:1460–7.